Deformation and stress behavior analysis of high concrete dam under the effect of reservoir basin deformation

Dongjian Zheng[1,2], Yanxin Xu[1,3], Meng Yang[*1], Hao Gu[1,3], Huaizhi Su[1,2], Xinbo Cui[4], and Erfeng Zhao[1,3]

[1]*State Key Laboratory of Hydrology-Water Resources and Hydraulic Engineering,
Hohai University, Nanjing, China*
[2]*College of Water Conservancy and Hydropower Engineering, Hohai University, Nanjing, China*
[3]*National Engineering Research Center of Water Resources Efficient Utilization and Engineering Safety,
Hohai University, Nanjing, China*
[4]*Information Center of land and resources in binzhou city, Binzhou, China*

Abstract. According to deformation data measured in some high concrete dams, for dam body deformation, there is a complex relationship with dam height and water head for different projects, instead of a simple monotonic relationship consistently. Meanwhile, settlement data of some large reservoirs exhibit a significant deformation of reservoir basin. As water conservancy project with high concrete dam and large storage capacity increase rapidly these decades, reservoir basin deformation problem has gradually gained engineers' attentions. In this paper, based on conventional analytical method, an improved analytical method for high concrete dam is proposed including the effect of reservoir basin deformation. Though establishing FEM models of two different scales covering reservoir basin and near dam area respectively, influence of reservoir basin on dam body is simulated. Then, forward and inverse analyses of concrete dam are separately conducted with conventional and proposed analytical methods. And the influence of reservoir basin deformation on dam working behavior is evaluated. The results of two typical projects demonstrate that reservoir basin deformation will affect dam deformation and stress to a certain extent. And for project with large and centralized water capacity ahead of dam site, the effect is more significant than those with a slim-type reservoir. As a result, influence of reservoir basin should be taken into consideration with conducting analysis of high concrete dam with large storage capacity.

Keywords: reservoir basin deformation; project with high dam and large storage capacity; high concrete dam; forward and inverse analysis; an improved analytical method

1. Introduction

With the development of water conservancy and hydropower construction, there have been a number of concrete dam projects with more than 200m in height and large storage capacity constructed or under construction in southwest China, which cause worldwide attention (Zhou *et*

---

*Corresponding author, Ph.D., E-mail: ymym_059@126.com

Table 1 High concrete dam projects of China in recent years

Name	Type	River	Dam height (m)	Capacity ($10^8 m^3$)	Hydropower installation (MW)
Jinping I	arch dam	Yalong	305	77.6	3600
Xiaowan	arch dam	Lancang	294.5	151	4200
Xiluodu	arch dam	Jinsha	285.5	128	14400
Longtan	gravity dam	Hongshui	216.5	273	6300
Songta	arch dam	Salween	313	45.5	3600
Baihetan	arch dam	Jinsha	289	188	14000
Longpan	arch dam	Jinsha	276	371	4200
Wudongde	arch dam	Jinsha	265	76	8700

Table 2 Maximum measured deformation of several high concrete arch dams in China

Name	Thickness-height ratio	Dam height (m)	Maximum base width (m)	Capacity ($10^8 m^3$)	Temperature condition	Maximum displacement (mm)
Longyangxia	0.45	178	80	240	Low	15.7
Geheyan	0.5	151	75	34	Low	19.79
Baishan	0.425	149.5	63.7	64	Low	61.68
Lijiaxia	0.29	155	45	16.5	Low	22.45
Linhekou	0.28	96.5	27.2	1.47	Low	34
Shimen	0.31	88	27.3	1.05	Low	28
Laxiwa	0.196	250	49	10.79	Low	61.95
Ertan	0.23	240	55.74	58	Low	121

al. 2006; Su *et al*. 2011; Yang and Liu 2015). As listed in Table 1, these projects are characterized with huge installed capacity, which will bring tremendous economic and social benefits. For the limited experience of key technologies for such projects with super high dam and large storage capacity, the safety problem during construction and operation process has gained extensive and close attention from engineers and experts.

In the dam body of these projects, different kinds of monitoring instruments are arranged. Among different monitoring quantities, deformation is characterized with high precision and simple measurement, which can reflect the overall dam working behavior. As a result, deformation is regarded to be the most important indicator of dam safety monitoring (Sortis and Paoliani 2007; Yang *et al*. 2015). Deformation of dam body in the operational process is caused by different load factors, such as water pressure, temperature load and seepage in the foundation, and is also related to factors as storage capacity, reservoir shape, geological conditions and dam boy shape (Finozzi *et al*. 2015). In general, a project with higher dam height and water head means larger water loading on dam body, which will lead to larger dam deformation as factors as dam body shape, topographic and geologic conditions and temperature condition are the same or similar (Mazars and Grange 2015).

According to the projects listed in Table 2, it is obvious that dam deformation does not always illustrate a generally-supposed monotonic relationship with dam height and water head. The dam

(a) Xiaowan(water level:1235m)

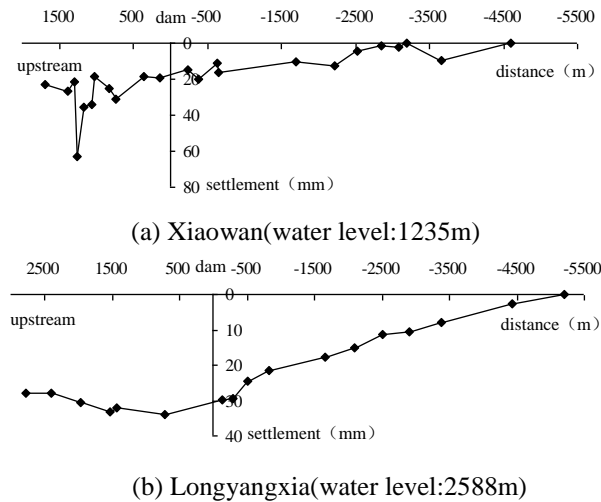(b) Longyangxia(water level:2588m)

Fig. 1 Reservoir basin settlement distribution

with higher height and water head will have smaller deformation for the comparison of Longyangxia and Geheyan under similar other factors. The abnormal discipline also applies to the comparison of Lijiaxia and Linhekou. In order to study this special deformation phenomenon, engineering experts analyzed the measured reservoir basin deformation of some typical projects and recognized that it was hugely related to the above abnormal dam deformation. As shown in Figs. 1(a)-(b), reservoir basin deformation causes the rotation of dam foundation and toppling deformation of dam body in the upstream direction. Meanwhile, effect of reservoir basin deformation varies for projects with different reservoir shapes and storage capacities. As a result, in order to accurately grasp the dam working behavior for those with high dam and huge storage capacity, there is a need to clarify the impact of reservoir basin deformation on concrete dam deformation and stress, which is significant for effective dam safety monitoring (Ren *et al*. 2007).

At the present stage, reservoir basin deformation problems have gained more and more attentions in real engineering projects, while monitoring and analysis jobs of reservoir basin deformation have been carried out for few of reservoir projects worldwide. Engineers have not yet formed a clear understanding of the impact of reservoir basin deformation on dam working behavior. On the contrary, a number of researches and discussions related to reservoir basin deformation problems have been conducted until now. For the parameter inversion problem, taking the effect of reservoir basin deformation into account, Gu and Wu (2006) proposed a deterministic model method to obtain mechanical parameters of dam body, dam foundation and reservoir basin. Gu *et al*. (2015) proposed an inverse analysis method for high concrete dam based on Chaos Genetic Optimization Algorithm. About the FEM analysis problem, the simulation method of stress and displacement boundary conditions is discussed in FEM analysis of gravity dam (Su *et al*. 2012). Then, the reservoir foundation is simplified as a semi-infinite body and studied the reasonable modeling scope and boundary constraint of FEM model (Su *et al*. 2014). About the reservoir basin deformation and its effect, Zhao *et al*. (2013) introduced the rule and influence factors of reservoir basin deformation by establishing several simplified models of different reservoir shape. Combining with engineering examples of earth rock dam, gravity dam and arch dam, Altunisik and Sesli (2015) developed the influence of the reservoir basin deformation on dam

deformation and stress with simplified calculation method. The deformation regularity and rheological behavior of Hoover reservoir basin are studied by analyzing the long-term settlement data (Pituba 2015). Generally, in the existing research, the forward and inverse analysis method of dam and reservoir basin, with the influence of reservoir basin deformation, was established. And general law and qualitative analysis of the reservoir basin deformation phenomenon and its influence on the dam deformation and stress were summarized. However, these methods are not so convenient or practical that they have not been applied to real engineering projects to provide the actual extent of reservoir basin influence. In this paper, a new practical method to study the effect of reservoir basin deformation is proposed. By establishing FEM models of two different scales including reservoir basin and near dam area and then applying reservoir basin deformation to the boundary of near dam area model, then effect of reservoir basin deformation is finally simulated. In case study section, two typical high-dam projects with different reservoir types are taken as examples to study the effects on dam deformation and stress quantitatively. By contrasting the results of conventional and proposed analytical methods, it can provide a scientific basis to establish a reasonable method to analyze working behavior for high concrete dam project with large reservoir capacity.

2. Analytical method of working behavior for high concrete dam under the effect of reservoir basin deformation

2.1 dam body deformation under the effect of water pressure

In the impounding and operational process of a reservoir, effect of reservoir water on dam-reservoir system has two parts: the pressure on dam surface and the water weight in reservoir basin. At any location of dam body, displacements generated by reservoir water, δ_H, are combinations of the effect of the two load parts. According to different generation mechanism, δ_H can be divided into dam-deformation component δ_{1H}, base-deformation component δ_{2H} and reservoir-deformation component δ_{3H} (Gu and Wu 2006). The pressure on dam surface leads to the deformation of dam and foundation, where δ_{1H} is the pure deformation of dam body and δ_{2H} is driven by the deformation of dam foundation. The water weight in reservoir basin leads to the settlement of reservoir area, which is the cause of δ_{3H}. As shown in Fig. 2, taking the
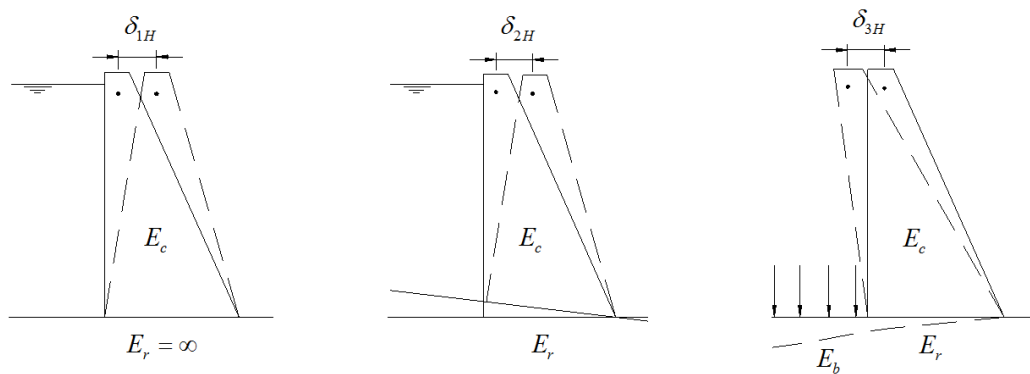

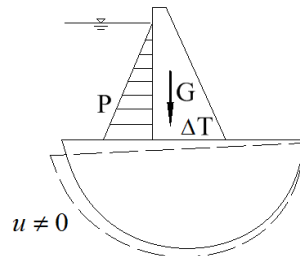Fig. 2 Schematic diagram of δ_{1H}, δ_{2H} and δ_{3H}

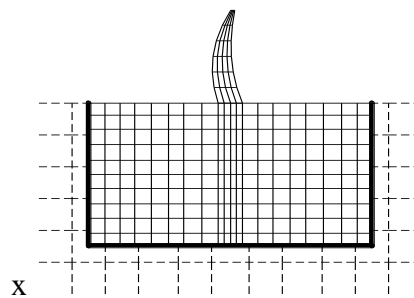Fig. 3 Load factors and boundary condition of near-dam area

Fig. 4 Mesh schematic of near-dam area and reservoir basin models

displacement along the river as an example, δ_{1H} and δ_{2H} are in downstream direction while δ_{3H} is in upstream direction.

E_c, E_r and E_b denote the elastic modulus of dam body, dam foundation and reservoir basin respectively. Set E_r to be 10 times more than E_c, regarding the dam foundation as a rigid body, then δ_{1H} can be obtained by applying water pressure on dam surface to FEM model of near-dam area. When E_c and E_r are real, δ_{2H} is obtained by subtracting δ_{1H} from dam deformation under water pressure load on dam surface. And δ_{3H} can be obtained by applying water pressure load on reservoir basin to a large-scale FEM model, on condition that E_c, E_r and E_b are real.

2.2 Effect analysis method of the reservoir basin deformation

Varied from the conventional structural analysis of dam body, foundation rock outside near-dam area is no longer thought to be fixed when effect of reservoir basin deformation is taken into consideration. Apart from the influence factors like water pressure load, dam gravity load and temperature load, the entire near-dam area is also within the displacement field of reservoir basin. Therefore, as shown in Fig. 3, scale of FEM model should cover the large reservoir area, rather than the conventional 2-3 times of dam height. And effect of reservoir basin deformation should be included in both forward and inverse analyses of dam structure.

In a project with high dam and large reservoir capacity, submerged area in the reservoir often reaches tens or even hundreds of kilometers. The dam body is a micro-structure within the vast reservoir area. Therefore, it is necessary to study the reservoir basin area and dam body in different scale to ensure the analytical accuracy. In this article, to study the effect of reservoir basin deformation on high concrete dam, FEM models of two different scales, including the vast reservoir area and the relatively small near-dam area, are established. Then linear elastic finite

element analysis is conducted. The analysis procedure is roughly divided into two steps: firstly, apply water pressure on the reservoir basin surface in the large-scale model to obtain the displacement field of reservoir basin; then, take the reservoir basin deformation as the boundary condition of the small-scale model to simulate its effect on dam structure.

The relative position of near-dam area and reservoir basin models are shown in Fig. 4. The solid-line meshes are elements of near-dam area model, while dotted-line meshes are elements of reservoir basin model. Thick lines represent the boundary of near-dam area. Interpolate nodes on the boundary in reservoir basin displacement field to obtain the boundary condition of near-dam area and apply it to the small-scale model to calculate the effect of reservoir basin deformation.

2.3 Establishment method of FEM model

2.3.1 Reservoir basin model of large scale
<u>*To determine the modeling scope*</u>
The modeling scopes of reservoir basin are composed of 5 parts: upstream, downstream, foundation depth, left bank and right bank. The reasonable values of the 5 scopes are determined by a number of trial calculations. Gradually increase the scale of a certain boundary, while the rest ones are fixed to be large enough. When the dam deformation comes to converge or is no longer affected by the type of boundary condition, it can be considered that the model boundary scope has reached a reasonable value.

<u>*Simplification of geological conditions*</u>
In the wide range of reservoir basin area, geological conditions and geological structures are too complicated to achieve an authentic and detailed simulation. To simplify the geological conditions, reservoir basin is divided by the main geological zoning in the horizontal range and bedrock is divided by the main geological stratification in depth direction. Meanwhile, important geological structures, major faults and fracture zones in the reservoir area need to be considered to simulate the truncation of reservoir deformation. The material parameters of each geological division can be determined according to the geological prospecting data or by inverse analysis with reservoir settlement data.

<u>*Choice of element size*</u>
To limit the number of elements and ensure the computational efficiency, different parts of reservoir model need to be with different simulation accuracy (Gu *et al*. 2002). As riverbed is directly loaded by water pressure, its simulation accuracy greatly influences the calculation results. Therefore, the element size within a certain range from the riverbed is relatively small, from 100 to 200m. With the increase of the distance from riverbed, element size can enlarge to 400 or 800m.

<u>*Boundary condition and load*</u>
For the reservoir basin model, bottom boundary condition is fixed constraint and the others are normal constraint. And load is the water pressure on reservoir basin surface.

2.3.2 Near-dam area model of small scale
To ensure the calculation accuracy of dam structure, detailed simulation of the topography, geological conditions and dam structure in the near-dam area is necessary. Boundary scope of the near-dam area model follows the conventional analysis method. As the minimum modeling scope,

take 2 times of dam height for the upstream scope and foundation depth, 1 time of dam height for left bank, right bank and downstream scope.

3. Inverse analysis method of elastic modulus for high concrete dam with large storage capacity

For newly built concrete dams, mechanical properties of concrete material will develop significantly during the early stage and tend to be stable gradually. After long-term operation, dam will produce aging and damage as the effect of environmental and loading factors. Therefore, the real elastic modulus of dam body always obviously varies from the original design or early test value (Sevim *et al.* 2014). In order to accurately grasp the dam working state so as to effectively monitor the dam safety, it is important to do inverse analysis with measured deformation data to obtain the true elastic modulus of dam body (Feng *et al.* 2004).

The inversion analysis of elastic modulus is to correct the assumptive value with dam displacement under obvious fluctuation of water level and corresponding finite element calculation results, as shown in Eq. (1).

$$E_c^{'} = K \times E_c = \frac{\Delta \delta_{1H}}{\Delta \delta_{1H}^{'}} \times E_c \tag{1}$$

where E_c and $E_c^{'}$ are assumptive and real elastic modulus of dam body; K is correction coefficient; δ_{1H} and $\delta_{1H}^{'}$ are calculative and real values of dam displacement; Δ indicates the change of displacement.

$\delta_{1H}^{'}$ is obtained by subtracting $\delta_{2H}^{'}$ and $\delta_{3H}^{'}$ from the actual water pressure component, δ_H. Conduct forward analysis of dam displacement with design value E_c and test or inversion value of $E_r^{'}$ and $E_b^{'}$. As $\delta_{2H}^{'}$ and $\delta_{3H}^{'}$ cannot be measured directly during engineering, it is necessary and reasonable to assume that $\delta_{2H}^{'}$ is equal to δ_{2H} and $\delta_{3H}^{'}$ is equal to δ_{3H}.

If the obvious fluctuation of water level takes a relative short period, as a fast impoundment process, influence of temperature change and aging on the dam displacement is pretty small and relatively backward. Therefore $\Delta \delta_H^{'}$ is the change of displacement measured in this condition. On the contrary, if the impoundment process is long, separation of water pressure component is required before the calculation of $\Delta \delta_H^{'}$.

As a consequence, the correction coefficient K to calculate the real elastic modulus of dam body is expressed as

$$K = \frac{\Delta \delta_{1H}}{\Delta \delta_H^{'} - \Delta \delta_{2H} - \Delta \delta_{3H}} \tag{2}$$

In the conventional inversion analysis method, effect of reservoir basin deformation is ignored that $\Delta \delta_{3H}$ is equal to 0. As $\Delta \delta_{3H}$ has an opposite sign with other displacement component, it means a larger inversion result for the conventional method.
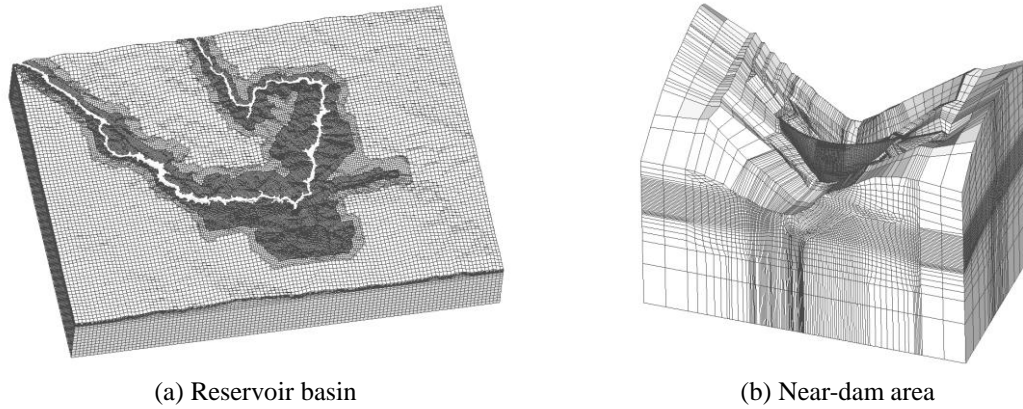
4. Case study

| (a) Reservoir basin | (b) Near-dam area |

Fig. 5 Finite element models of project I
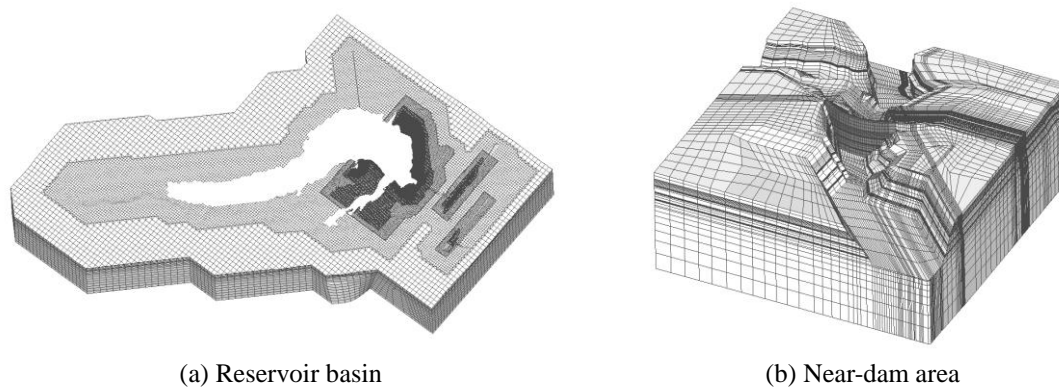

| (a) Reservoir basin | (b) Near-dam area |

Fig. 6 Finite element models of project II

4.1 Project situation

Project I, Xiaowan dam is a hyperbolic arch dam of 294.5 meters located in the southwest of China. The normal water level is 1240m and the corresponding reservoir capacity is 15 billion m^3. 2 kilometers in front of the dam site, the reservoir is divided into the 123km east branch and the 178km west branch. Steep mountains on both sides of the reservoir form a "V" shaped valley. Project II, Longyangxia dam is a gravity arch dam of 178 meters located in the northwest of China. Its normal water level is 2600m with a corresponding reservoir capacity of 24.7 billion m^3, while the maximum water level during reservoir operation is 2597.62m. The reservoir is 101km long with an area of 383km^2. The valley ahead the dam is "V" shape and the water surface expands rapidly to a maximum 9km in the upstream.

4.2 Establishment of FEM models

According to the aforementioned modeling methods and principles, finite element models of reservoir basin and near-dam area are established for project I and II, as shown in Figs. 5(a)-(b) and 6(a)-(b). The modeling scopes of reservoir basin are shown in Table 3.

Table 3 Modeling scopes of reservoir basin model (km)

	Upstream	Downstream	Left bank	Right bank	Depth
Project I	44	21	40	50	11
Project II	70	17	16	20	10

Table 4 Material parameters E_r of each geological division for reservoir basin model

	Project I				Project II		
Zone	Layer	Depth range(m)	Elastic modulus(GPa)	Zone	Layer	Depth range(m)	Elastic modulus(GPa)
1	1	0~40	2.5	1	1	0~30	8
	2	40~140	13		2	30~100	14
	3	140~440	25		3	100~10000	20
	4	440~11000	35	2	1	0~300	1
2	1	0~40	2		2	300~1000	1.5
	2	40~140	8		3	1000~2000	14
	3	140~440	18		4	2000~10000	20
	4	440~11000	26	Faultage	1	0~30	2.8
Faultage	1	0~300	1		2	30~300	3.5
	2	300~800	3			/	

Table 5 Material parameters E_b of each geological division for near-dam area model

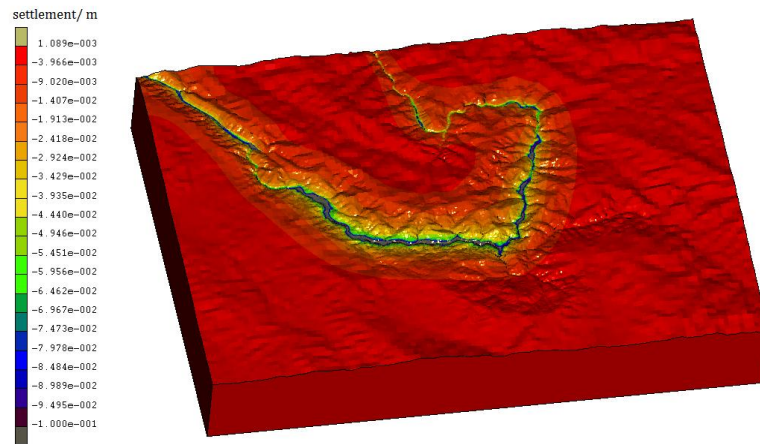| Project I		Project II	
Rock category	Elastic modulus(GPa)	Rock category	Elastic modulus(GPa)
I	25	I	20
II	20	II	16
III	10	III	8
Faultage	0.3	Faultage	2.7

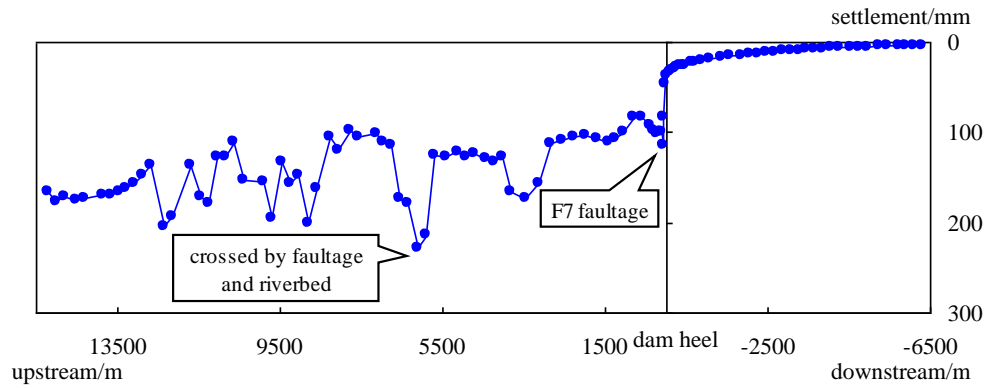Fig. 7 Nephogram of Xiaowan reservoir basin settlement(water level:1240m)

Fig. 8 Settlement distribution of river bed for Xiaowan reservoir(water level:1240m)
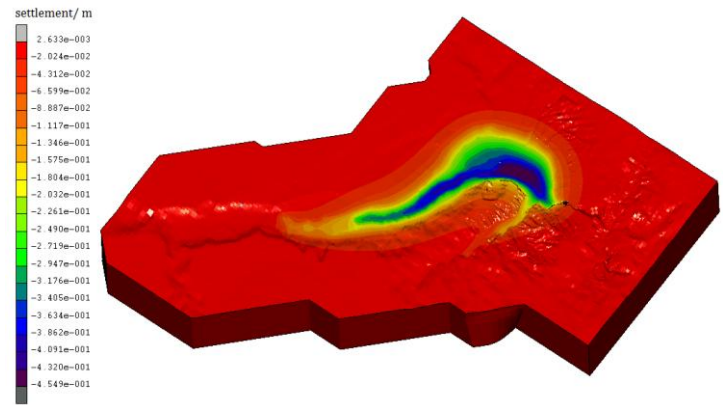

Fig. 9 Nephogram of Longyangxia reservoir basin settlement(water level:2597.62m)

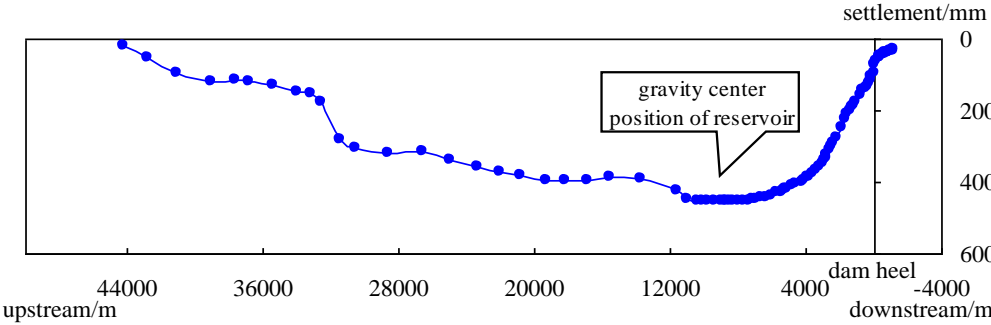Fig. 10 Settlement distribution of river bed for Longyangxia reservoir(water level:2597.62m)

Based on geological prospecting data of reservoir area and near-dam area, E_r of reservoir basin model and E_b of near-dam area model for project I and project II are shown in Tables 4-5.

4.3 Deformation of reservoir basin

Nephogram of reservoir basin settlement for project I and II under highest water level were

shown in Figs. 7 and 9. Settlement distribution of river bed along the main river, from 6.5km downstream to 15km upstream in the west branch for project I and from 1.2km downstream to 45km upstream for project II, were shown in Figs. 8 and 10 with a reversed scale value of vertical axis.

It can be seen from the figures that settlement occurs in submerged area, as well as mountains and downstream area within a certain range of the reservoir. And the location farther from the reservoir has a smaller settlement. Settlement of dam heel is significantly larger than that of downstream area, which indicates the rotation of foundation in the upstream direction. In project I, large settlement occurs in the river bed where there is deep water, wide water surface or a crossing fault. The maximum settlement, 228.7mm, occurs 6.1km from the dam site. In project II, water surface is gradually becoming wide and there is no significant geological structure or weak area, therefore distribution of riverbed settlement is smooth. In the gravity center position of reservoir, 9.3km from the dam site, the maximum settlement reaches 454.6mm.

4.4 Inverse analysis of elastic modulus for dam body

According to actual operation process of project I, denote water level 1165m as the base water level as the dam grouting finished, and four characteristic levels within a storage period are
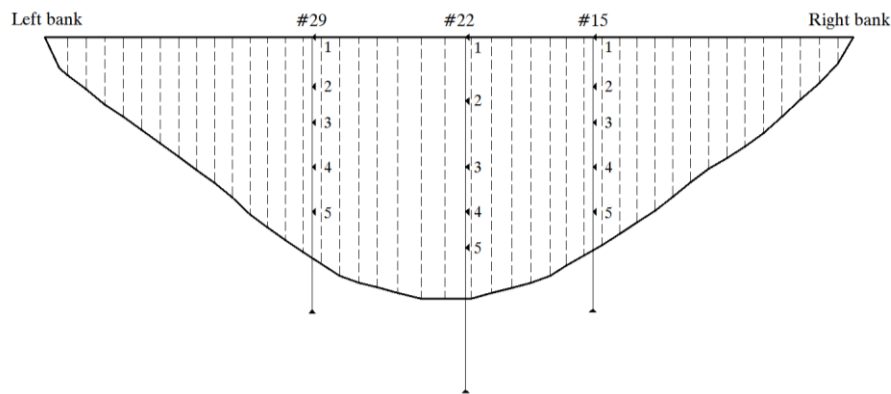

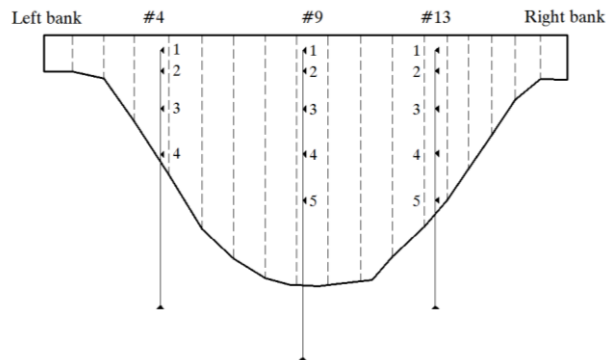Fig. 11 Measure points layout in the dam body for project I

Fig. 12 Measure points layout in the dam body for project II

Table 6 Displacement component δ_{1H} of arch crown beam under characteristic water level

Measure point	Project I					Project II			
	1165m	1181m	1225m	1233m	1240m	2534m	2560m	2562m	2593m
1	42.95	57.73	116.48	131.47	145.99	0.89	6.51	7.24	26.76
2	43.33	57.05	106.20	117.54	128.14	0.93	6.23	6.91	24.33
3	42.00	53.00	87.25	94.41	100.93	1.02	5.75	6.32	19.93
4	35.87	43.67	66.19	70.72	74.79	1.07	4.76	5.17	13.63
5	25.91	30.66	43.83	46.40	48.71	0.88	2.71	2.89	6.39

Table 7 Displacement component δ_{2H} of arch crown beam under characteristic water level(mm)

Measure point	Project I					Project II			
	1165m	1181m	1225m	1233m	1240m	2534m	2560m	2562m	2593m
1	1.52	1.97	3.37	3.77	3.97	0.75	1.01	1.02	1.41
2	1.16	1.51	2.61	2.86	3.01	0.68	0.91	0.93	1.28
3	0.89	1.19	1.94	2.14	2.29	0.57	0.76	0.78	1.08
4	0.68	0.88	1.43	1.63	1.73	0.44	0.60	0.61	0.85
5	0.47	0.62	1.02	1.12	1.17	0.31	0.42	0.43	0.60

Table 8 Displacement component δ_{3H} of arch crown beam under characteristic water level(mm)

Measure point	Project I					Project II			
	1165m	1181m	1225m	1233m	1240m	2534m	2560m	2562m	2593m
1	-3.38	-4.02	-6.07	-6.48	-6.85	-5.23	-7.04	-7.16	-9.88
2	-2.62	-3.12	-4.72	-5.04	-5.32	-4.75	-6.4	-6.51	-8.99
3	-1.88	-2.25	-3.41	-3.65	-3.86	-3.96	-5.35	-5.45	-7.55
4	-1.4	-1.67	-2.55	-2.73	-2.89	-3.09	-4.18	-4.26	-5.92
5	-1.01	-1.21	-1.85	-1.98	-2.1	-2.19	-2.97	-3.03	-4.22

1181m, 1225m, 1233m and 1240m respectively. For project II, denote water level 2534m as the base water level and the gradually rising water levels in the next few years as analytical water levels, which are 2560m, 2562m and 2593m respectively. Displacement components δ_{1H}, δ_{2H} and δ_{3H} under each water level were calculated with original design of elastic modulus for project I and II, 25GPa and 20GPa respectively.

Several vertical lines are arranged in the dam body for the two projects and the layout of measuring points are shown in Figs. 11-12. Taking displacement of arch crown beam(dam section 22 for project I and dam section 9 for project II) as an example, the three displacement components of different measure points are listed in Tables 6-8. For project I, the maximum effect of reservoir basin deformation on dam displacement is 6.85mm in the dam crest under water level 1240m. For project II, the maximum effect is 9.88mm under water level 2593m. As listed in Table 9, water pressure component is separated from measured displacement with statistical model(In the statistical model, δ_H' is set to be zero at base water level for the two projects). With the above

Table 9 Displacement component $\delta_H^{'}$ of arch crown beam under characteristic water level(mm)

Measure point	Project I					Project II			
	1165m	1181m	1225m	1233m	1240m	2534m	2560m	2562m	2593m
1	0	16.14	66.92	85.92	104.28	0	4.78	4.34	18.41
2	0	18.33	59.7	73.87	86.93	0	4.22	3.65	15.95
3	0	16.65	44.15	53.73	61.95	0	4.42	3.78	12.62
4	0	13.91	34.93	43.21	50.75	0	2.02	1.39	6.77
5	0	6.04	15.8	18.71	21.49	0	2.78	1.85	4.49

Table 10 Radial displacement increment of arch crown beam relative to 1165m for project I(mm)

Measure point	$\Delta\delta_{1H}$				$\Delta\delta_{1H}^{'}$			
	1181m	1225m	1233m	1240m	1181m	1225m	1233m	1240m
1	14.78	73.53	88.52	103.04	16.33	67.76	86.77	105.30
2	13.72	62.88	74.21	84.82	18.48	60.35	74.59	87.78
3	11.00	45.25	52.42	58.93	16.72	44.63	54.25	62.53
4	7.79	30.32	34.85	38.92	13.98	35.33	43.59	51.19
5	4.74	17.91	20.49	22.79	6.09	16.09	19.03	21.88

Table 11 Radial displacement increment of arch crown beam relative to 2534m for project II(mm)

Measure point	$\Delta\delta_{1H}$			$\Delta\delta_{1H}^{'}$		
	2560m	2562m	2593m	2560m	2562m	2593m
1	5.61	6.35	25.86	6.33	5.99	22.4
2	5.29	5.98	23.39	5.63	5.16	19.58
3	4.72	5.31	18.91	5.61	5.06	15.7
4	3.68	4.09	12.55	2.95	2.39	9.2
5	1.83	2.01	5.5	3.45	2.57	6.23

displacement components in Tables 6-9, $\Delta\delta_{1H}$ and $\Delta\delta_{1H}^{'}$ of each measure point are calculated, as shown in Tables 10-11.

Here we have two sequences of $\Delta\delta_{1H}$ and $\Delta\delta_{1H}^{'}$ for each project. According to Eqs. (1)-(2), there is a linear relationship between $\Delta\delta_{1H}$ and $\Delta\delta_{1H}^{'}$ as $\Delta\delta_{1H}=K\times\Delta\delta_{1H}^{'}$. Therefore, a comprehensive adjustment coefficient K can be obtained by data fitting work with the two sequences to represent the elastic modulus of whole dam body. For project I and II, they are 1.05 and 1.15 respectively. Thereby, the inversed elastic modulus $E_c^{'}$ are 26.25GPa and 23.0GPa. When the effect of reservoir basin deformation is not considered and $\Delta\delta_{3H}$ is set to be 0 in Eq. (2), the comprehensive adjustment coefficients are 1.13 and 1.31. And the corresponding $E_c^{'}$ are 28.25GPa and 26.2GPa. As a result, after the consideration of reservoir basin deformation, the inversion results of elastic modulus are reduced by 2.0GPa and 3.2GPa respectively.

(a) Project I	(b) Project II

Fig. 13 Schematic diagram of displacement of crown cantilever dam section by reservoir basin deformation(wireframe represents the undeformed dam)

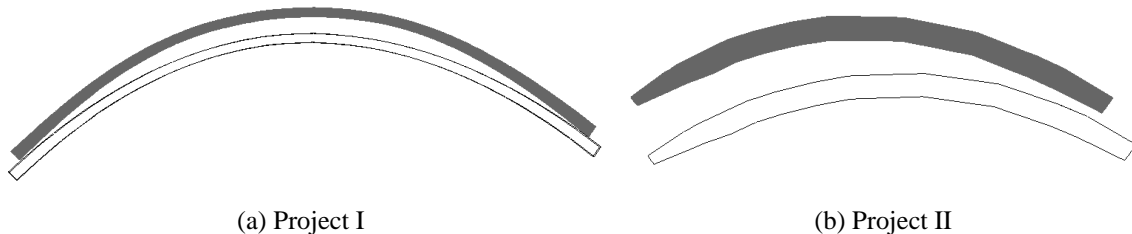|	
(a) Project I	(b) Project II

Fig. 14 Schematic diagram of horizontal displacement of dam crest by reservoir basin deformation (wireframe represents the undeformed dam)

4.5 Analysis of dam working behavior

With elastic modulus from the proposed and conventional inversion methods, deformation and stress state of high concrete dam were calculated under water pressure for project I and II. To establish the reasonable analytic method of dam structure behavior for project with high dam and large storage capacity, the effect of reservoir basin deformation on dam working behavior is evaluated. For project I and II, dam working behavior is analyzed under the normal water level 1240m and the maximum operating water level 2597m.

4.5.1 Deformation behavior

Apply reservoir basin deformation on boundary nodes of near-dam area model, and the corresponding displacement of dam body are shown in Figs. 13(a)-(b) and 14(a)-(b). Under the effect of reservoir basin, a phenomenon is illustrated, settlement and toppling deformation in the upstream direction. For project I, dam displacements of left and right bank are symmetrical on the whole, and the maximum displacement is emerged in the arch crown beam. For project II, water load is mainly concentrated on the right side in front of dam and displacements on right bank are larger than those on left bank.

Under the effect of water pressure on dam surface and reservoir basin deformation, radial displacements of vertical points for the two dams are shown in Tables 12-13. The total radial displacement of riverbed dam section is larger than that of bank slope dam section, which corresponds to the general rule of arch dam deformation. The maximum displacements of the two

Table 12 Dam radial displacement for project I (mm)

Dam section	Measure point	Method 1 δ_H	Effect of reservoir basin δ_{3H}	$\left\|\dfrac{\delta_{3H}}{\delta_H}\right\| \times 100\%$	Method 2 δ_H	Effect of parameter variation $\Delta(\delta_{1H}+\delta_{2H})$
15 (right bank)	1	106.93	-4.57	4.27	104.04	7.46
	2	89.33	-3.64	4.07	86.94	6.03
	3	73.59	-2.93	3.98	71.76	4.75
	4	50.36	-2.04	4.05	49.53	2.88
	5	26.24	-1.25	4.76	26.42	1.07
22 (river bed)	1	131.75	-6.45	4.90	128.25	9.95
	2	112.15	-5.00	4.46	108.86	8.29
	3	83.63	-3.59	4.29	81.39	5.83
	4	58.22	-2.68	4.60	57.21	3.68
	5	35.67	-1.97	5.52	35.78	1.86
29 (left bank)	1	97.62	-5.23	5.36	95.52	7.33
	2	82.16	-4.07	4.95	80.28	5.94
	3	68.20	-3.25	4.77	66.75	4.70
	4	47.36	-2.26	4.77	46.70	2.92
	5	25.96	-1.40	5.39	26.14	1.22

dams are 131.75mm and 27.29mm. For project I, at the crest of crown cantilever dam section, effect of reservoir basin on the dam displacement reaches the maximum 6.45mm. Overall, the effect of reservoir basin accounts for about 4% of total dam displacement, and the maximum is 5.52%. For project II, at the crest of dam section 13th on the right bank, effect of reservoir basin reaches the maximum 12.3mm. The effect is obvious for the whole dam, of which the maximum is 3 times more than total dam displacement.

For the proposed analysis method and conventional analysis method (hereinafter referred to as method 1 and method 2), the consideration of reservoir basin effect and the different inversed elastic moduli of dam concrete account for the difference of total displacement in two methods. In method 1, consideration of the reservoir basin deformation will reduce dam total displacement in downstream direction while the smaller inversed elastic modulus will lead to larger results. As shown in Tables 12-13, effects of the two factors on dam displacement have a same distribution law with a larger displacement at a higher measure point while they have opposite effects on the total displacement in method 1. For project I, the two effects are very close as magnitude on the whole and effect of elastic modulus variation is slightly larger (except for the 5th measuring points on each vertical line of low elevation). Therefore with method 1, most measuring points are with a slightly larger total displacement δ_H than method 2, and the maximum displacement change is 3.50mm, accounting for 2.66% of δ_H. For project II, the effect of reservoir basin deformation is significantly larger than that of elastic modulus variation. As a result, δ_H of each measuring point is larger in method 2, and the maximum displacement change is 10.77mm, accounting for 103.7% of δ_H.

Table 13 Dam radial displacement for project II (mm)

Dam section	Measure point	Method 1 δ_H	Effect of reservoir basin δ_{3H}	$\left\|\dfrac{\delta_{3H}}{\delta_H}\right\| \times 100\%$	Method 2 δ_H	Effect of parameter variation $\Delta(\delta_{1H}+\delta_{2H})$
4 (left bank)	1	7.94	-3.45	43.45	10.92	0.47
	2	7.11	-3.11	43.74	9.81	0.42
	3	5.28	-2.53	47.92	7.55	0.27
	4	2.73	-1.88	68.86	4.55	0.06
9 (river bed)	1	27.29	-10.52	38.55	34.96	2.86
	2	25.25	-9.59	37.98	32.22	2.62
	3	21.45	-8.05	37.53	27.32	2.18
	4	16.00	-6.30	39.38	20.74	1.56
	5	9.94	-4.48	45.07	13.51	0.91
13 (right bank)	1	10.38	-12.30	118.50	21.15	1.52
	2	9.56	-11.07	115.79	19.26	1.37
	3	7.74	-9.09	117.44	15.75	1.08
	4	4.83	-6.88	142.44	11.03	0.67
	5	1.40	-4.66	332.86	5.83	0.23

(a) Stress in beam direction of upstream face

(b) Stress in beam direction of downstream face

(c) Stress in arch direction of upstream face

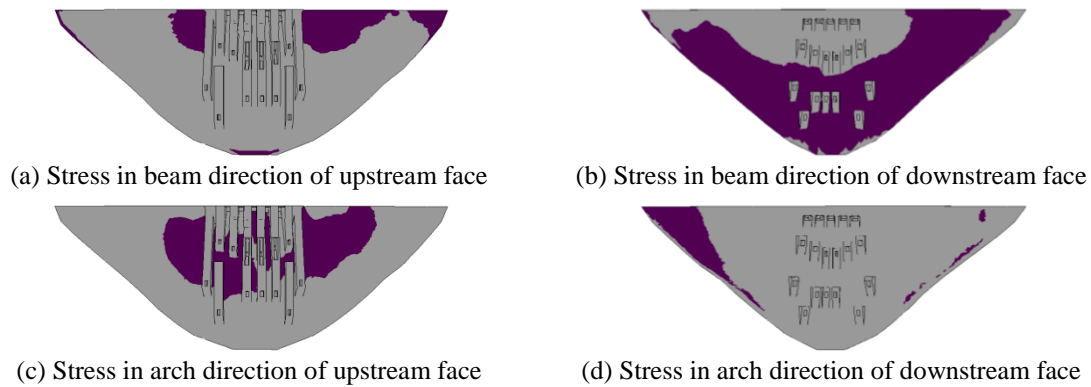(d) Stress in arch direction of downstream face

Fig. 15 Dam stress for project I under the effect of reservoir basin deformation (shadow part is tensile region and gray part is compression region)

4.5.2 Stress behavior

Apply reservoir basin deformation on boundary nodes of near-dam area model for project I, and the tensile and compression region for stress in arch and beam direction are shown in Figs. 15(a)-(d) (Shadow part represents tensile region). The tensile region of stress in beam direction are located in dam heel of riverbed dam section, upstream face of high elevation site for some dam sections and downstream face of middle and low elevation site for most dam sections. The tensile region of stress in arch direction appears in upstream face of central part for arch rings of middle and high elevation and downstream face of arch abutment.
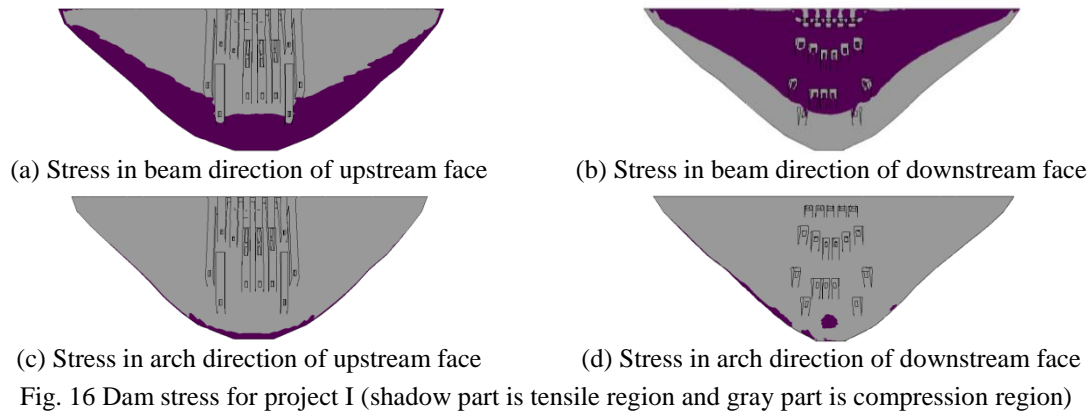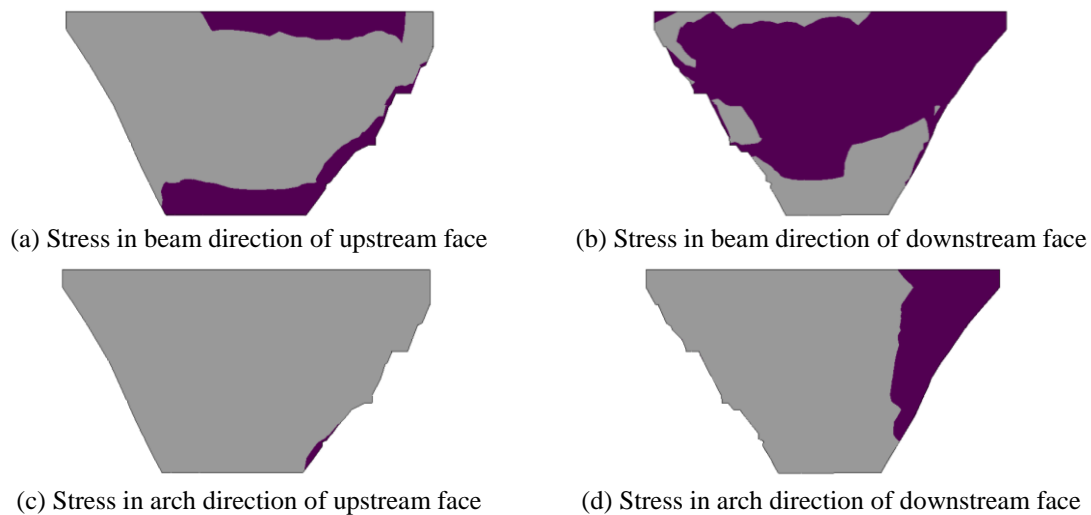
(a) Stress in beam direction of upstream face

(b) Stress in beam direction of downstream face

(c) Stress in arch direction of upstream face

(d) Stress in arch direction of downstream face

Fig. 16 Dam stress for project I (shadow part is tensile region and gray part is compression region)

Table 14 Extreme value of characteristic stress in project I (MPa)

Stress	Method	Maximum tensile stress	Maximum compressive stress
	Effect of reservoir basin	0.03	0.43
In arch direction	Method 1	0.18	10.76
	Method 2	0.17	11.09
	Effect of reservoir basin	0.12	0.10
In beam direction	Method 1	8.54	10.17
	Method 2	7.78	9.58

(a) Stress in beam direction of upstream face

(b) Stress in beam direction of downstream face

(c) Stress in arch direction of upstream face

(d) Stress in arch direction of downstream face

Fig. 17 Dam stress for project II under the effect of reservoir basin deformation (shadow part is tensile region and gray part is compression region)

With method 1, tensile and compression region for stress in arch and beam direction are shown in Figs. 16(a)-(d). The tensile region of stress in beam direction is located in upstream face of low elevation site and downstream face of middle and high elevation site for each dam section (Figs.

(a) Stress in beam direction of upstream face

(b) Stress in beam direction of downstream face

(c) Stress in arch direction of upstream face

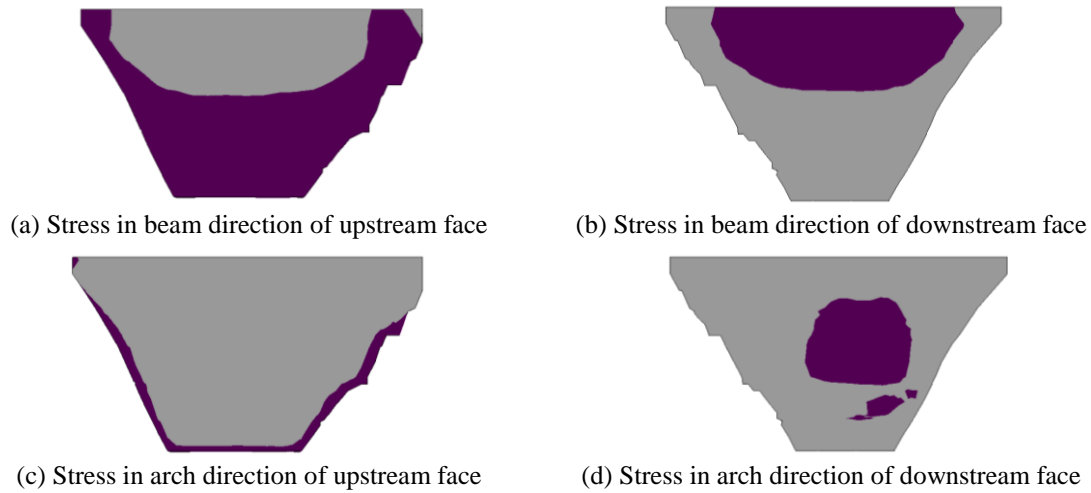(d) Stress in arch direction of downstream face

Fig. 18 Dam stress for project II (shadow part is tensile region and gray part is compression region)

16(a)-(b)). The tensile region of stress in arch direction appears in upstream and downstream face of arch abutment for arch rings of middle and low elevation and downstream face of arch crown for arch rings of low elevation (Figs. 16(c)-(d)). With method 2, tensile and compression region for dam stress is in agreement with that in method 1.

Characteristic value of dam stress for project I is shown in Table 14. The effect of reservoir basin deformation is -0.43～0.03MPa on stress in arch direction and -0.10～0.12MPa on stress in beam direction, accounting for a small ratio of the actual stress in method 1. The position and the value of extremum stress are very close in method 1 and method 2.

Under the effect of reservoir basin deformation for project II, tensile and compression region for stress in arch and beam direction are shown in Figs. 17(a)-(d) (Shadow part represents tensile region). The tensile region of stress in beam direction are located in dam heel of riverbed and right bank dam section, upstream face of high elevation site and downstream face of middle and high elevation site for most dam sections. The tensile region of stress in arch direction appears in upstream face of right abutment for arch ring near dam base and downstream face of left abutment for arch rings of middle and high elevation.

With method 1, tensile and compression region for stress in arch and beam direction are shown in Figs. 18(a)-(d). The tensile region of stress in beam direction is located in upstream face of middle and low elevation site for each dam section and downstream face of middle and high elevation site for riverbed dam section (Figs. 18(a)-(b)). The tensile region of stress in arch direction appears in upstream face of arch abutment for arch rings of middle and low elevation and downstream face of arch crown for arch rings of middle elevation (Figs. 18(c)-(d)). With method 2, tensile and compression region for dam stress is similar to that in method 1, the tensile region of stress in beam direction on upstream face and stress in arch direction on downstream face have certain development in high and low elevation direction respectively.

Characteristic value of dam stress for project II is shown in Table 15. The effect of reservoir basin deformation is -1.28～0.58MPa on stress in arch direction and -0.22～0.35MPa on stress in beam direction, accounting for a large ratio of the actual stress in method 1. The positions of extremum stress are very close in method 1 and method 2 while the value is significantly different.

Table 15 Extreme value of characteristic stress in project II (MPa)

Stress	Method	Maximum tensile stress	Maximum compressive stress
	Effect of reservoir basin	0.58	1.28
In arch direction	Method 1	2.80	2.67
	Method 2	3.42	3.35
	Effect of reservoir basin	0.35	0.22
In beam direction	Method 1	3.62	2.04
	Method 2	4.33	2.90

4.5.3 Evaluation of the effect of reservoir basin deformation

According to above results, reservoir basin deformation has a certain degree of influence on dam deformation and stress. For project I, reservoir basin deformation has an effect of about 5% of actual dam displacement while for project II the effect is more significant, about 300% to the maximum. And the effect on dam stress has a similar feature. With reservoir basin deformation taken into consideration, forward and inverse analysis results also differ from that of conventional analytical method. The variation is also slight for project I and significant for project II. To sum up, relative to project I, reservoir basin deformation has a much greater effect on dam working behavior in project II. Therefore, it cannot be neglected in the analysis of dam working state.

By comparing specific engineering situation of two projects, we can know that the effect degree of reservoir basin deformation is related to reservoir types to a great extent. In project I, the reservoir is slim and is divided into two branches about 2 km in the upstream. For project II, the water surface expands rapidly to a maximum 9km in the upstream. In contrast, there is a larger storage capacity and more centralized water load in a certain scope ahead of dam in project II. Also, the effect has something to do with geological conditions in reservoir area. With relatively weaker rock stiffness on the whole, reservoir basin will have a larger deformation for project II. As a result of the two factors, the reservoir basin deformation has a more significant effect on dam deformation and stress in project II.

5. Conclusion

In this paper, an improved analytical method for high concrete dam is proposed including the effect of reservoir basin deformation. FEM models of two different scales are established and influence of reservoir basin on dam body is simulated. Based on the theoretical and experimental study, the following conclusions are drawn:

• Reservoir basin deformation is a common phenomenon in reservoir project. Under the effect of water pressure, reservoir basin has a larger settlement in the upstream and smaller settlement in the downstream. It leads to toppling deformation of dam body in the upstream direction.

• By establishing FEM models of two different scales including reservoir basin and near dam area respectively, influence of reservoir basin on dam working state is simulated. With this method, the forward and inverse analysis results of dam working state are more accordant with actual situation.

• Reservoir basin deformation has a certain effect on both displacement and stress of concrete dam. The forward and inverse analysis results with effect of reservoir basin are also different with

that of the conventional method. Calculation results show that reservoir basin deformation will have a significant effect on concrete dam for high dam project with wide water surface and centralized water load in a reservoir with weak rock stiffness.

   • For project with high dam and large storage capacity, reservoir basin has an obvious deformation phenomenon. In the forward and inverse analysis of concrete dam, it is necessary to clarify the impact of reservoir basin deformation. It helps to select a reasonable analytical method and achieve an accurate grasp of dam working state.

Acknowledgments

References

Altunisik, A.C. and Sesli, H. (2015), "Dynamic response of concrete gravity dams using different water modelling approaches: Westergaard, lagrange and euler", *Comput. Concrete*, **16**(3), 429-448.

Finozzi, I.B.N., Berto, L. and Saetta, A. (2015), "Structural response of corroded RC beams: a comprehensive damage approach", *Comput. Concrete*, **15**(3), 411-436.

Feng, X., Zhou, J. and Fan, Y.F. (2004), "Inverse analysis of concrete dam with modal measurements", *J. Hydraul. Eng*, **2,** 101-105.

Gu, C.S., Zheng, D.J. and Wu, Z.R. (2002), "Precision analysis on simulational finite element model of dam and batholith", *Hydroelec. Energy*, **20**(2), 13-16.

Gu, C.S. and Wu, Z.R. (2006), *Safety Monitoring of Dams and Dam Foundations - Theory, Methods and Their Application*, Press of Hohai University, Nanjing, China.

Gu, H., Wu, Z.R. and Huang, X.F. (2015), "Zoning modulus inversion method for concrete dams based on chaos genetic optimization algorithm", *Math. Probl. Eng.*, 1-9.

Mazars, J. and Grange, S. (2015), "Modeling of reinforced concrete structural members for engineering purposes", *Comput. Concrete*, **16**(5), 683-701.

Pituba, J.J.C. (2015), "A damage model formulation: Unilateral effect and RC structures analysis", *Comput. Concrete*, **15**(5), 709-733.

Ren, Q.W., Xu, L.Y. and Wan, Y.H. (2007), "Research advance in safety analysis methods for high concrete dam", *Sci. China. Ser. E.*, **50**(1), 62-78.

Sevim, B., Altunisik, A.C. and Bayraktar, A. (2014), "Construction stages analyses using time dependent material properties of concrete arch dams", *Comput. Concrete*, **14**(5), 599-612.

Sortis, A.D. and Paoliani, P. (2007), "Statistical analysis and structural identification in concrete dam monitoring", *Eng. Struct*, **29**(1), 110-120.

Su, H.Z., Hu, J. and Li, J.Y. (2012), "Deep stability evaluation of high-gravity dam under combining action of powerhouse and dam", *Int. J. Geomech*, **13**(3), 257-272.

Su, H.Z., Li, J.Y. and Cao, J.P. (2014), "Macro-comprehensive evaluation method of high rock slope stability in hydropower projects". *Stoch. Env. Res. Risk. A*, **28**(2), 213-224.

Su, H.Z., Wen, Z.P. and Wu, Z.R. (2011). "Study on an intelligent inference engine in early-warning system of dam health", *Water. Resour. Manag.*, **25**(6),1545-1563.

Yang, M. and Liu, S. (2015), "Field tests and finite element modeling of a Prestressed Concrete Pipe pile-composite foundation", *J. Civ. Eng.*, **19**(7), 2067-2074.

Yang, M., Su, H.Z. and Yan, X.Q. (2015), "Computation and analysis of high rocky slope safety in a water conservancy project", *Discrete. Dyn. Nat. Soc.*, 1-11.

Zhao, E.F., Zhang, L.Z. and Wu, B.B. (2013), "Influencing factors of high arch dam operating status with the action effect of reservoir basin", *Disaster. Adv.*, **6**(3), 107-111.

Zhou, J.P., Yang, Z.Y. and Chen, G.F. (2006), "Status and challenges of high dam constructions in China", *J. Hydraul. Eng.*, **37**(12), 1433-1438.

CC